Role of LBPA and Alix in Multivesicular Liposome Formation and Endosome Organization

Hirotami Matsuo,[1]* Julien Chevallier,[1] Nathalie Mayran,[1] Isabelle Le Blanc,[1] Charles Ferguson,[3] Julien Fauré,[4] Nathalie Sartori Blanc,[5] Stefan Matile,[2] Jacques Dubochet,[5] Rémy Sadoul,[4] Robert G. Parton,[3] Francis Vilbois,[6] Jean Gruenberg[1]†

What are the components that control the assembly of subcellular organelles in eukaryotic cells? Although membranes can clearly be distorted by cytosolic factors, very little is known about the intrinsic mechanisms that control the biogenesis, shape, and organization of organellar membranes. Here, we found that the unconventional phospholipid lysobisphosphatidic acid (LBPA) could induce the formation of multivesicular liposomes that resembled the multivesicular endosomes that exist where this lipid is found in vivo. This process depended on the same pH gradient that exists across endosome membranes in vivo and was selectively controlled by Alix. In turn, Alix regulated the organization of LBPA-containing endosomes in vivo.

Membranes and vesicles accumulate within multivesicular or multilamellar endosomes along the degradation pathway leading to lysosomes, and these selectively incorporate some proteins, including down-regulated receptors for growth factors and hormones (*1*, *2*). In late endosomes, LBPA [or bis(monoacylglycero)phosphate] is abundant in these internal membranes, accounting for ≈15 mole percent of total organelle phospholipids (*3*). LBPA has not been detected elsewhere in the cell and is involved in protein and lipid trafficking through late endosomes (*3*–*7*).

We synthesized 2,2′-dioleoyl LBPA (*8*) (Fig. 1, A and B), the major isoform (>90%) in baby hamster kidney (BHK) cells (*9*), and we prepared large liposomes (*10*) with a phospholipid composition similar to that of late endosomes (dioleoylphosphatidylcholine: dioleoylphosphatidylethanolamine: phosphatidylinositol:LBPA, 5:2:1:2 mol) (*3*, *9*). When labeled with the fluorescent dye FM2-10, large unilamellar liposomes (diameters of ≈600 to 800 nm) were easily revealed by light microscopy, whether LBPA was present (Fig. 1C) or not present (Table 1). Because the late endosomal lumen is acidic (pH 5.0 to 5.5) (*1*), we mimicked this situation in vitro by incubating lipids at pH 5.5 during the phase reversion of the liposome assembly process; the external pH was then neutralized to reproduce the pH gradient formed in vivo (*10*). Liposomes lacking LBPA remained unilamellar (Fig. 1D and Table 1), whereas LBPA liposomes showed 5 to 10 internal vesicles (Fig. 1E and Table 1), thus resembling multivesicular regions of the late endosomes that were observed by electron microscopy (EM) (*3*, *9*, *11*, *12*). Internal vesicles were also observed within LBPA-

Table 1. MVLs. Liposomes were prepared at pH 5.5 or 7.4, or they were prepared at pH 7.4 and then the internal pH was switched to pH 5.5 (*10*). After labeling with FM 2-10, an aliquot of the assay mixture was mounted onto a coverslip (final volume = 3 μl), and the number (*n*) of MVLs was counted (*10*). About 300 liposomes from three independent experiments were counted for each condition. Data are also expressed as a percentage (%) of the number of MVLs in the presence of 2,2′-LBPA and a pH gradient. pH in, liposome pH; pH out, external pH; aLBPA Ab, antibody to LBPA; IC AB, isotypic control antibody. ND, not determined.

	pH in/pH out = 5.5/7.4		pH in/pH out = 7.4/7.4	
	n	%	*n*	%
Liposomes prepared at pH 5.5 or pH 7.4				
2,2′-dioleoyl LBPA	91	100	2	2
Control (no LBPA)	4	4	3	3
2,2′-dioleoyl LBPA + aLBPA Ab	4	4	ND	ND
2,2′-dioleoyl LBPA + IC AB	74	81	ND	ND
3,3′-dioleoyl LBPA	17	19	3	3
3,3′-dimyristoyl LBPA	2	2	4	4
Trimyristoyl semi-LBPA	1	1	1	1
Trioleoyl semi-LBPA	4	4	1	1
Liposomes prepared at pH 7.4 and then switched to pH 5.5				
2,2′-dioleoyl LBPA	107	100	ND	ND
Control (no LBPA)	15	14	ND	ND
2,2′-dioleoyl LBPA + aLBPA Ab	10	10	ND	ND
2,2′-dioleoyl LBPA + IC AB	64	60	ND	ND

[1]Department of Biochemistry, [2]Department of Organic Chemistry, University of Geneva, 30 quai Ernest Ansermet, 1211 Geneva 4, Switzerland. [3]Institute for Molecular Bioscience, Center for Microscopy and Microanalysis and School of Biomedical Sciences, University of Queensland, Queensland 4072, Australia. [4]Neurodégénérescence et Plasticité Inserm–Université Joseph Fourier, Hôpital A. Michallon, 38043 Grenoble Cedex 9, France. [5]Laboratoire d'Analyse Ultrastructurale, University of Lausanne, 1015 Lausanne, Switzerland. [6]Serono Pharmaceutical Research Institute, 1228 Plan-les-Ouates, Switzerland.

*Present address: Department of Chemical Pharmacy, Shujitsu University, 1-6-1 Nishigawara, Okayama 703–8516, Japan.

†To whom correspondence should be addressed. E-mail: jean.gruenberg@biochem.unige.ch

containing liposomes (Fig. 1G), but not control liposomes (Fig. 1F), by cryo-EM of vitreous sections, in which the specimen is thought to be a faithful representation of the original material (*13*, *14*).

Multivesicular liposomes (MVLs) failed to form in the absence of a pH gradient or when the luminal pH was less acidic (pH ≥6), as it is in early or recycling endosomes. In LBPA, oleoyl chains are predominantly esterified to the thermodynamically unstable β position of the glycerol backbone (2,2′-LBPA, shown in Fig. 1A) in vivo, and fatty acids can migrate to the α positions (3,3′-LBPA) (*8*, *9*). MVL formation was substantially reduced when we used other LBPA isoforms (Table 1), including 3,3′-LBPA, or semi-LBPA, a triple acylated isoform found in the vaccinia virus and perhaps in the Golgi complex (*15*, *16*) (Table 1). Thus, 2,2′-LBPA, the major late endosomal isoform, is endowed with the intrinsic capacity to stimulate internal vesicle formation within acidic liposomes and thus to generate structures that resemble late endosomes.

To follow the bilayer invagination process, liposomes were prepared at neutral pH and then acidified by incubation at pH 5.5 with the protonophore nigericin. After drug removal by rapid chromatography and neutralization of the external pH, liposomes were incubated with the water-soluble dye 8-hydroxypyrene-1,3,6-trisulfonic acid (HPTS).

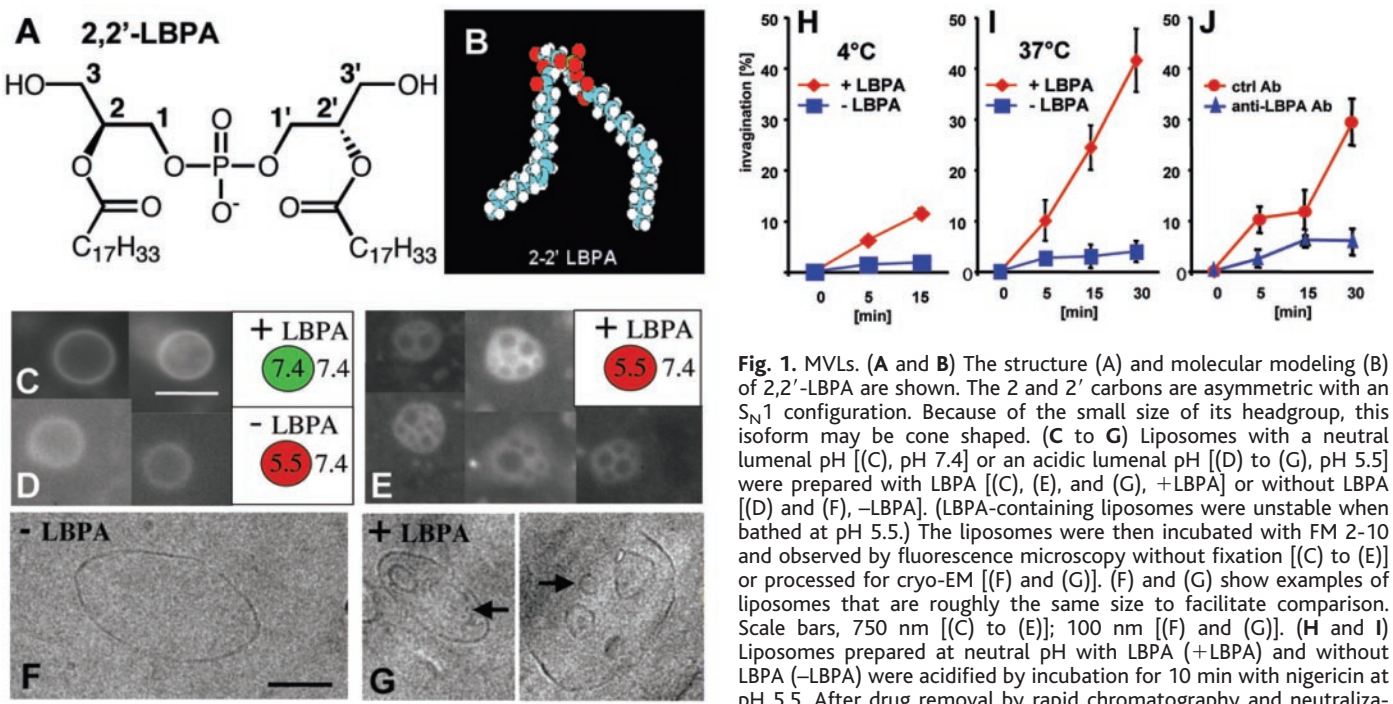

Fig. 1. MVLs. (**A** and **B**) The structure (A) and molecular modeling (B) of 2,2′-LBPA are shown. The 2 and 2′ carbons are asymmetric with an S_N1 configuration. Because of the small size of its headgroup, this isoform may be cone shaped. (**C** to **G**) Liposomes with a neutral lumenal pH [(C), pH 7.4] or an acidic lumenal pH [(D) to (G), pH 5.5] were prepared with LBPA [(C), (E), and (G), +LBPA] or without LBPA [(D) and (F), –LBPA]. (LBPA-containing liposomes were unstable when bathed at pH 5.5.) The liposomes were then incubated with FM 2-10 and observed by fluorescence microscopy without fixation [(C) to (E)] or processed for cryo-EM [(F) and (G)]. (F) and (G) show examples of liposomes that are roughly the same size to facilitate comparison. Scale bars, 750 nm [(C) to (E)]; 100 nm [(F) and (G)]. (**H** and **I**) Liposomes prepared at neutral pH with LBPA (+LBPA) and without LBPA (–LBPA) were acidified by incubation for 10 min with nigericin at pH 5.5. After drug removal by rapid chromatography and neutralization of the milieu, liposomes were incubated with HPTS at 4°C (H) or 37°C (I). After quenching external HPTS with DPX, the fluorescence intensity of HPTS entrapped within liposomes was quantified. For each condition, the mean ± SEM of three experiments is shown. Upon prolonged incubations (>30 min), LBPA liposomes became unstable and showed a tendency to aggregate. (**J**) LBPA liposomes were switched to an acidic pH, as in (H) and (I), but 3 μg/ml of the antibody to LBPA or isotypic control antibody (ctrl Ab) was added together with HPTS. For each condition, the mean ± SEM of three experiments is shown.

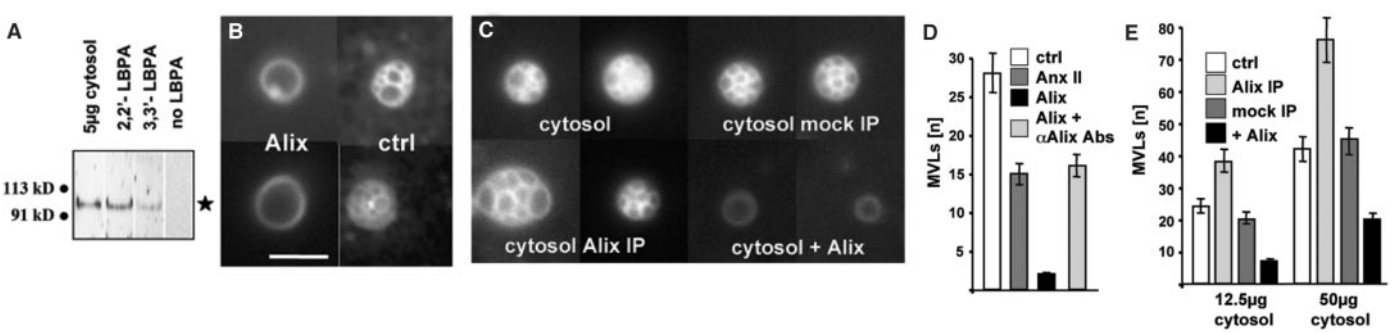

Fig. 2. Alix-dependent MVL formation. (**A**) Liposomes containing 2,2′-LBPA or 3,3′-LBPA, or lacking LBPA (no LBPA), were incubated in 250 μg of complete cytosol in the presence of a pH gradient (as in Fig. 1, H and I), retrieved by floatation in gradients, and then analyzed by Western blotting with antibodies to Alix. A lane loaded with 5 μg of cytosol is shown for comparison. The star marks the position of Alix. (**B**) 2,2′-LBPA liposomes were prepared at a neutral pH, and switched to pH 5.5, as in Fig. 1H (ctrl, control), or incubated with 5 μg purified recombinant Alix or annexin II (Anx II). Lipid concentrations and buffer solutions were identical to those in (C) and (E) (with cytosol) to facilitate comparison. Scale bar, 750 nm. (**C**) Liposomes prepared as in (B) were incubated in 50 μg of cytosol, or cytosol immunodepleted with 5 μg of rabbit antibody to Alix (cytosol Alix IP), mock treated with 5 μg of rabbit immunoglobulin G (cytosol mock IP), or complemented with 5 μg of purified Alix (cytosol + Alix). (B) and (C) show examples of liposomes that are roughly the same size to facilitate comparison. (**D**) The number (*n*) of MVLs in (B) was counted, as in Table 1. MVLs were also quantified after the addition of both Alix and antibodies to Alix (αAlix Abs). Different experimental conditions [see (B)] account for different values of *n* in the control here and in Table 1. (**E**) Liposomes were incubated in 12.5 or 50 μg of complete cytosol, as in (C), and MVLs were quantified, as in (D). In (D) and (E), more than 300 liposomes from three independent experiments were counted.

Then, the dye remaining in the external milieu was quenched selectively with p-xylene-bis-pyridinium bromide (DPX) (*10*, *17*). Liposomes containing LBPA showed a highly significant capacity to incorporate HPTS at both 4°C (>10% of the liposome volume) and 37°C (≈5.75 μl/μmol lipid or ≈40% of the liposome volume) when compared with controls lacking LBPA (<4% of the liposome volume) (Fig. 1, H and I, and Table 1). These liposomes also retained the capacity to form MVLs (Table 1), much like liposomes prepared at pH 5.5 (Fig. 1E). In addition, an antibody against LBPA (*3*), but not an isotypic control antibody, inhibited the invagination process (Fig. 1J) and MVL formation (Table 1), confirming the role of LBPA in the formation of intraliposomal vesicles. Similarly, the antibody prevented the formation of MVLs that were prepared at pH 5.5 when it was present during the pH neutralization step (Table 1). Thus, the invagination process can be reconstituted upon acidification of LBPA-containing liposomes, which mimics the endosome acidification that occurs in vivo.

In vivo, the formation (and dynamics) of internal membranes within late endosomes is presumably controlled by proteins. After incubation in cytosol, we found that five proteins were selectively recruited onto LBPA liposomes, but not control liposomes. One of these proteins was identified by tandem mass spectrometry as Alix, a cytosolic partner of ALG-2 (*18*), which is also present in exosomes (*19*) and phagosomes (*20*). The yeast homolog of Alix, Vps31p (also known as Bro1p or Npi3p), is involved in multivesicular endosome biogenesis, perhaps in concert with or downstream of the endosomal sorting complex III required for transport (ESCRT-III) (*21*). Moreover, Alix interacts with ESCRT proteins and, similar to ESCRT proteins, plays a role in human immunodeficiency virus budding at the plasma membrane (*22*, *23*).

Cytosolic Alix was preferentially recruited by liposomes containing 2,2′-dioleoyl LBPA (2,2′-LBPA) when it was compared with liposomes lacking LBPA or containing 3,3′-LBPA (Fig. 2A). Without cytosol, purified recombinant Alix (*24*) strongly inhibited MVL formation (Fig. 2, B and D) without affecting the liposomal pH, and this inhibition was partially reversed by antibodies to Alix (Fig. 2D). The phospholipid-binding protein annexin II (*25*), used as a control, reduced MVL formation, but to a much lesser extent than did Alix (Fig. 2D). Although cytosol supported MVL formation efficiently in a dose-dependent manner (Fig. 2, C and E), excess purified Alix inhibited MVL formation. Conversely, Alix immunodepletion

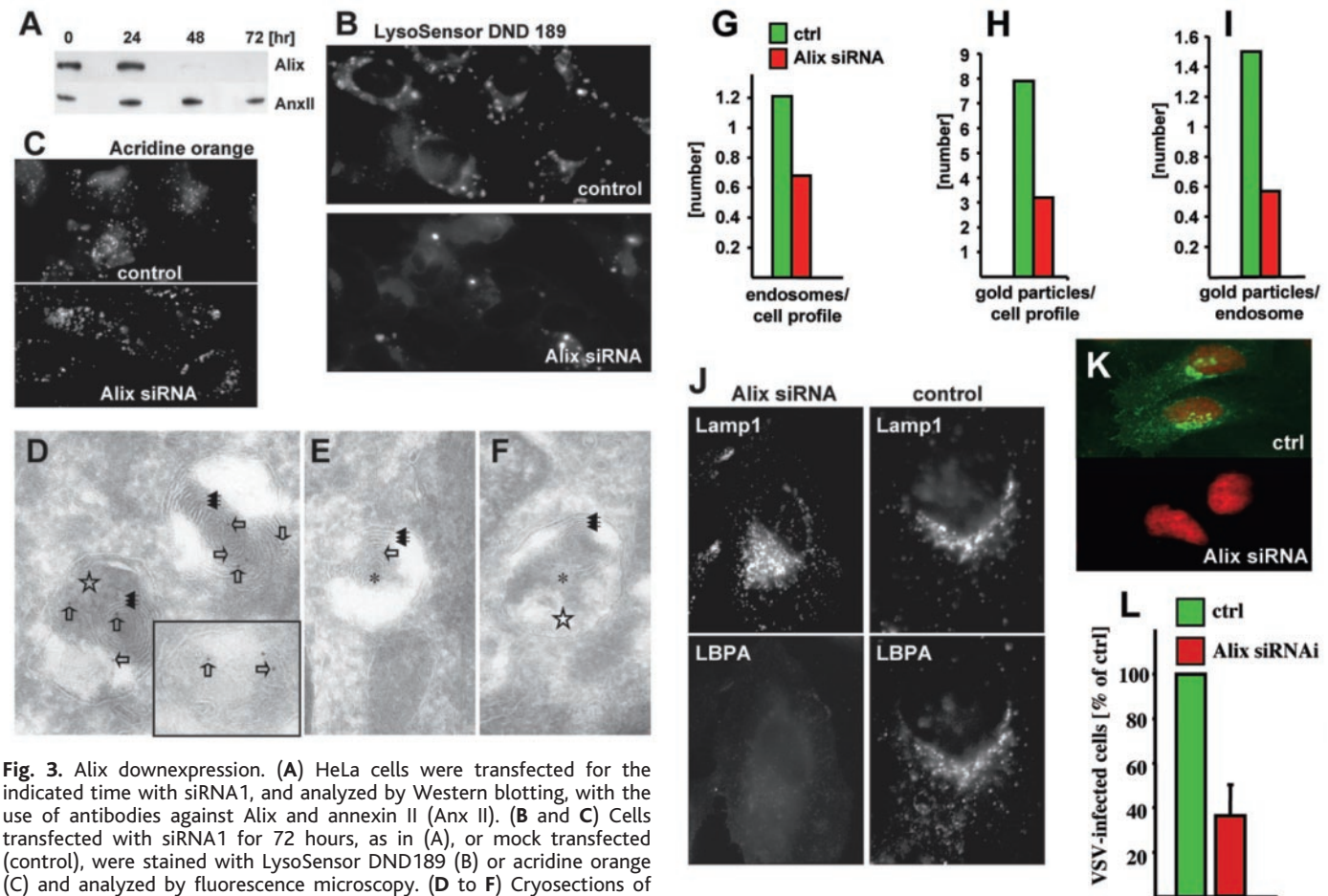

Fig. 3. Alix downexpression. (**A**) HeLa cells were transfected for the indicated time with siRNA1, and analyzed by Western blotting, with the use of antibodies against Alix and annexin II (Anx II). (**B** and **C**) Cells transfected with siRNA1 for 72 hours, as in (A), or mock transfected (control), were stained with LysoSensor DND189 (B) or acridine orange (C) and analyzed by fluorescence microscopy. (**D** to **F**) Cryosections of cells transfected with Alix siRNA1 [(E) and (F)] or mock transfected (D) were immunogold labeled with antibodies to LBPA. Open arrows point at gold particles; black triple arrows and stars indicate multilamellar and vesicular regions, respectively; asterisks show late endosomes in siRNA-treated cells with a typical multilamellar/multivesicular morphology but devoid of labeling. (**G** to **I**) The total number of multilamellar late endosomes (G), the total number of gold particles per cellular profiles (H), and the number of gold particles per late endosomal profiles (I) were quantified in 35 flat cell profiles selected at random, each section containing a nuclear profile. (**J**) Alix siRNA1-treated cells and mock-transfected cells were analyzed by indirect immunofluorescence with antibodies against LBPA and Lamp1. (**K** and **L**) Cells transfected with Alix siRNA1 or mock transfected were infected with VSV for 3 hours, labeled with antibodies against the glycoprotein G (G protein) of VSV and fluorescein isothiocyanate–labeled secondary antibodies (green), and analyzed by immunofluorescence (K); cells are identified by nuclear staining (red). In control infected cells (ctrl), the newly synthesized VSV–G protein is abundant in the endoplasmic reticulum and the Golgi complex, whereas the number of infected cells is reduced by Alix siRNA1. The number of infected cells was quantified (L); data show the mean of three independent experiments.

from the cytosol markedly stimulated MVL formation, whereas control antibodies had no effect (Fig. 2, C and E).

When Alix expression was silenced by small interfering RNAs (siRNAs) in HeLa cells (Fig. 3A), the number of acidic, late endocytic compartments appeared to be reduced (based on a probe selective for pH values between 5 and 5.5; Fig. 3B), whereas the acidification properties of other organelles (such as early endosomes and the trans-Golgi network) seemed to be unaffected (based on a probe detecting less acidic pH; Fig. 3C). By EM, LBPA (Fig. 3, D and E, open arrows) was found in HeLa cells both in multilamellar regions (Fig. 3D, black triple arrow) and multivesicular regions (Fig. 3D, star and inset), frequently within the same late endosome. Consistently, Alix siRNAs reduced the number of late endosomes containing multilamellar regions (which could be unambiguously identified on sections) (Fig. 3B), whereas other organelles, including the Golgi complex, seemed to be unaffected (Fig. 3G).

A biochemical analysis showed that Alix downexpression reduced LBPA to ≈50% of that of the control. Consistently, the LBPA staining of Lamp1-positive late endosomes was decreased by immunofluorescence (Fig. 3J), as were the total number of anti-LBPA gold particles both per cell profile (Fig. 3H) and per late endosomes (Fig. 3, E and F, quantification in I) by EM. Vesicular stomatitis virus (VSV) infects cells from the endocytic pathway, but beyond early endosomes (*26*, *27*). The acidic endosomal pH triggers fusion of the VSV envelope with endosomal membranes, allowing nucleocapsid release into the cytoplasm. Viral infection (Fig. 3K, quantification in L) was inhibited by Alix downexpression, presumably because the number of acidic late endosomes was decreased. Alternatively, Alix-dependent dynamics of late endosomal membranes may be required for efficient nucleocapsid release.

We found that LBPA possesses the capacity to drive the formation of membrane invaginations within acidic liposomes. We also found that Alix controls this invagination process in vitro and the organization of LBPA-containing endosomes in vivo. We postulate that internal vesicles and the limiting membrane interact dynamically by means of fission and fusion events, and that the inward fission process is controlled, at least in part, by transient interactions between LBPA membranes and Alix (*28*), presumably together with other factors, including perhaps ESCRT proteins (*22*, *23*).

References and Notes

1. J. Gruenberg, *Nature Rev. Mol. Cell Biol.* **2**, 721 (2001).
2. D. J. Katzmann, G. Odorizzi, S. D. Emr, *Nature Rev. Mol. Cell Biol.* **3**, 893 (2002).
3. T. Kobayashi *et al.*, *Nature* **392**, 193 (1998).
4. B. Galve de Rochemonteix *et al.*, *Arterioscler. Thromb. Vasc. Biol.* **20**, 563 (2000).
5. J. P. Incardona, J. Gruenberg, H. Roelink, *Curr. Biol.* **12**, 983 (2002).
6. T. Kobayashi *et al.*, *Nature Cell Biol.* **1**, 113 (1999).
7. C. Lebrand *et al.*, *EMBO J.* **21**, 1289 (2002).
8. J. Chevallier *et al.*, *Org. Lett.* **2**, 1859 (2000).
9. T. Kobayashi *et al.*, *J. Biol. Chem.* **277**, 32157 (2002).
10. Materials and methods are available as supporting material on *Science* Online.
11. J. M. Escola *et al.*, *J. Biol. Chem.* **273**, 20121 (1998).
12. M. Kleijmeer *et al.*, *J. Cell Biol.* **155**, 53 (2001).
13. J. Dubochet *et al.*, *Q. Rev. Biophys.* **21**, 129 (1988).
14. J. Dubochet, N. Sartori Blanc, *Micron* **32**, 91 (2001).
15. E. B. Cluett, C. E. Machamer, *J. Cell Sci.* **109**, 2121 (1996).
16. E. B. Cluett, E. Kuismanen, C. E. Machamer, *Mol. Biol. Cell* **8**, 2233 (1997).
17. M. M. Tedesco, S. Matile, *Bioorg. Med. Chem.* **7**, 1373 (1999).
18. M. Missotten, A. Nichols, K. Rieger, R. Sadoul, *Cell Death Differ.* **6**, 124 (1999).
19. C. Thery *et al.*, *J. Immunol.* **166**, 7309 (2001).
20. J. Garin *et al.*, *J. Cell Biol.* **152**, 165 (2001).
21. G. Odorizzi, D. J. Katzmann, M. Babst, A. Audhya, S. D. Emr, *J. Cell Sci.* **116**, 1893 (2003).
22. U. K. von Schwedler *et al.*, *Cell* **114**, 701 (2003).
23. B. Strack, A. Calistri, S. Craig, E. Popova, H. G. Göttlinger, *Cell* **114**, 689 (2003).
24. C. Chatellard-Causse *et al.*, *J. Biol. Chem.* **277**, 29108 (2002).
25. N. Mayran, R. G. Parton, J. Gruenberg, *EMBO J.* **22**, 3242 (2003).
26. E. Daro, D. Sheff, M. Gomez, T. Kreis, I. Mellman, *J. Cell Biol.* **139**, 1747 (1997).
27. J. A. Whitney, M. Gomez, D. Sheff, T. E. Kreis, I. Mellman, *Cell* **83**, 703 (1995).
28. The possible roles of LBPA and Alix are discussed in the supporting online material text.

29. We thank M.-H. Beuchat for expert technical assistance, N. Sakai for her help with LBPA synthesis, and G. van der Goot for helpful comments. J.F. was supported by a fellowship from the French Ligua against Cancer. This work was supported by grants from the Human Frontier Science Programme Organization (J.G. and R.G.P.), the Swiss National Science Foundation (J.G. and J.D.), and the Australian National Health and Medical Research Council (R.G.P.).

Supporting Online Material

www.sciencemag.org/cgi/content/full/303/5657/531/DC1
Materials and Methods
SOM Text
References

9 October 2003; accepted 26 November 2003

Snapshots of DsbA in Action: Detection of Proteins in the Process of Oxidative Folding

Hiroshi Kadokura,[1] Hongping Tian,[1]* Thomas Zander,[2]† James C. A. Bardwell,[2] Jon Beckwith[1]‡

DsbA, a thioredoxin superfamily member, introduces disulfide bonds into newly translocated proteins. This process is thought to occur via formation of mixed disulfide complexes between DsbA and its substrates. However, these complexes are difficult to detect, probably because of their short-lived nature. Here we show that it is possible to detect such covalent intermediates in vivo by a mutation in DsbA that alters *cis* proline-151. Further, this mutant allowed us to identify substrates of DsbA. Alteration of the *cis* proline, highly conserved among thioredoxin superfamily members, may be useful for the detection of substrates and intermediate complexes in other systems.

The formation of disulfide bonds is essential for the folding, activity, and stability of many proteins exported from the cytoplasm. In both prokaryotes and eukaryotes, proteins with the thioredoxin fold are responsible for introducing disulfide bonds into substrate proteins (*1*–*3*). When a substrate protein appears in the periplasm of *Escherichia coli*, DsbA rapidly oxidizes it by donating the disulfide bond from its active site, Cys^{30}-Pro^{31}-His^{32}-Cys^{33}, to a pair of cysteines in the substrate (*4*–*7*). DsbA, in turn, is maintained in its oxidized form (*8*) by a membrane protein DsbB (*9*), which transfers electrons from DsbA to quinones in the respiratory chain using its four essential cysteines (*10*–*12*).

Substrate oxidation by DsbA likely begins with a deprotonated cysteine in the substrate attacking the disulfide bond in the active site of DsbA (*2*, *3*, *6*, *13*) (Fig. 1A). This reaction leads to the formation of a complex in which DsbA and the substrate are linked together by an intermolecular disulfide bond. In the next step, the mixed disulfide bond is attacked by a second deprotonated cysteine of the substrate to resolve the complex and release the oxidized substrate and the reduced DsbA. Although in vitro data are consistent with this model (*6*, *13*, *14*), the covalent reaction intermediate between DsbA and substrate has not

[1]Department of Microbiology and Molecular Genetics, Harvard Medical School, Boston, MA 02115, USA. [2]Department of Molecular, Cellular, and Developmental Biology, University of Michigan, Ann Arbor, MI 48109, USA.

*Present address: Harvard School of Public Health, Boston, MA 02115, USA.
†Present address: Profos Ag, Josef-Engert-Straβe 9, 93053 Regensburg, Germany.
‡To whom correspondence should be addressed. E-mail: jbeckwith@hms.harvard.edu